

WUE-ITP-2004-007  
DESY 04-030  
NSF-KITP-04-29  
February 2004

# Numerical evaluation of phase space integrals by sector decomposition

T. Binoth<sup>a</sup> and G. Heinrich<sup>b</sup>

<sup>a</sup>*Institut für Theoretische Physik und Astrophysik  
Universität Würzburg, Am Hubland, 97074 Würzburg, Germany*

<sup>b</sup>*II. Institut für theoretische Physik, Universität Hamburg,  
Luruper Chaussee 149, 22761 Hamburg, Germany*

## Abstract

In a series of papers we have developed the method of iterated sector decomposition for the calculation of infrared divergent multi-loop integrals. Here we apply it to phase space integrals to calculate a contribution to the double real emission part of the  $e^+e^- \rightarrow 2$  jets cross section at NNLO. The explicit cancellation of infrared poles upon summation over all possible cuts of a given topology is worked out in detail for a specific example.

# 1 Introduction

The precision measurements at LEP, SLAC, HERA and the Tevatron in the past years made it obvious that QCD corrections at next-to-leading order (NLO) accuracy are mandatory for a successful comparison of data and theory. Fortunately, a multitude of NLO corrections are available these days and the techniques for these calculations have reached a rather mature state, at least in what concerns  $1 \rightarrow 3$  or  $2 \rightarrow 2$  partonic processes.

However, the advent of the LHC and above all an  $e^+e^-$  linear collider will provide instances where the NLO QCD corrections are – in some particular cases – not sufficiently accurate to match the experimental precision. This is true for example for the extraction of the strong coupling constant  $\alpha_s$  from jet observables at a future  $e^+e^-$  collider.

This fact served as a motivation for substantial progress towards the calculation of NNLO corrections to important processes, in particular in what concerns the two-loop virtual corrections [1]–[6] and the one-loop corrections combined with real radiation where one additional parton is emitted [7, 8, 9]. The construction of a fully differential NNLO partonic Monte Carlo program however also requires the calculation of the real emission part where up to two partons can be unresolved, and – last but not least – the combination of all the ingredients to a stable and sufficiently fast Monte Carlo program. In what concerns the double real emission, subtraction schemes have been proposed in the literature [10, 11, 12], but a complete calculation including the final Monte Carlo program has been performed so far only for the particular case of the photon + jet– rate in  $e^+e^-$  annihilation [13, 14]. However, a lot of activity concerning this subject is going on at the moment. The efforts are concentrated particularly on the process  $e^+e^- \rightarrow 3$  jets, as this reaction is both appealing from a phenomenological point of view (e.g. measurement of  $\alpha_s$ ) as well as from a theoretical one (no problems due to initial state singularities). Nevertheless, it is worthwhile to consider first the reaction  $e^+e^- \rightarrow 2$  jets as this is the simplest example where the treatment of the double unresolved real radiation can be studied, and therefore a good testing ground for a new method.

Progress in what concerns the integration of subtraction terms has been made in [15], where it has been shown that the integrals of any  $1 \rightarrow 4$  matrix element in massless QCD over the total phase space can be expressed by four master integrals. These integrals have been evaluated analytically as well as numerically.

The complexity of the phase space integrals with two unresolved partons stems from the fact that the corresponding IR singularity structure is overlapping. We have demonstrated in [16] how one can disentangle in an automated way overlapping singularities in parameter representations of dimensionally regulated multi-loop integrals. The method of *iterated sector decomposition*, combined with numerical integration of the pole coefficients, proved successful to deal with very complicated Feynman diagrams [16, 17].

In this paper we apply the same ideas to parameter representations of phase space integrals, as a continuation of the work done in [15, 18]. In the same context the method of sector decomposition also has been applied meanwhile in [19].

In contrast to [15], where this method of numerical integration has been applied to master integrals only, we show here that we also can deal with numerators coming from gauge couplings and thus finally with complete matrix elements. Working through one example in great detail, we demonstrate the viability of our approach, showing explicitly

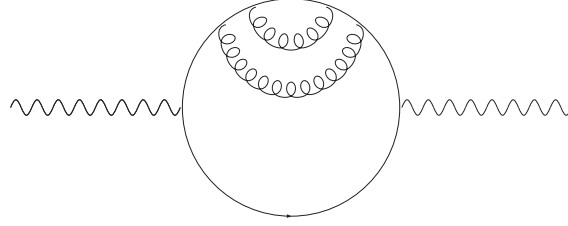


Figure 1: Sample three loop topology related to  $e^+e^- \rightarrow 2$  jets at NNLO.

the cancellation of infrared poles for a given topology when summing over all cuts.

The paper is organised as follows. In section 2 we discuss in detail the cancellation of infrared divergences in a concrete example. We work out the cut structure and the counterterms and represent the considered topology by a number of cut diagrams which give rise to phase space integrals. In section 3 we present the analytical results for the 2- and 3-particle cut diagrams, and in section 4 we discuss the method to perform the phase space integration of the 4-particle cut numerically. In section 5 we present the numerical result for a more complicated topology which has up to  $1/\epsilon^4$  poles. Section 6 closes the paper with a discussion.

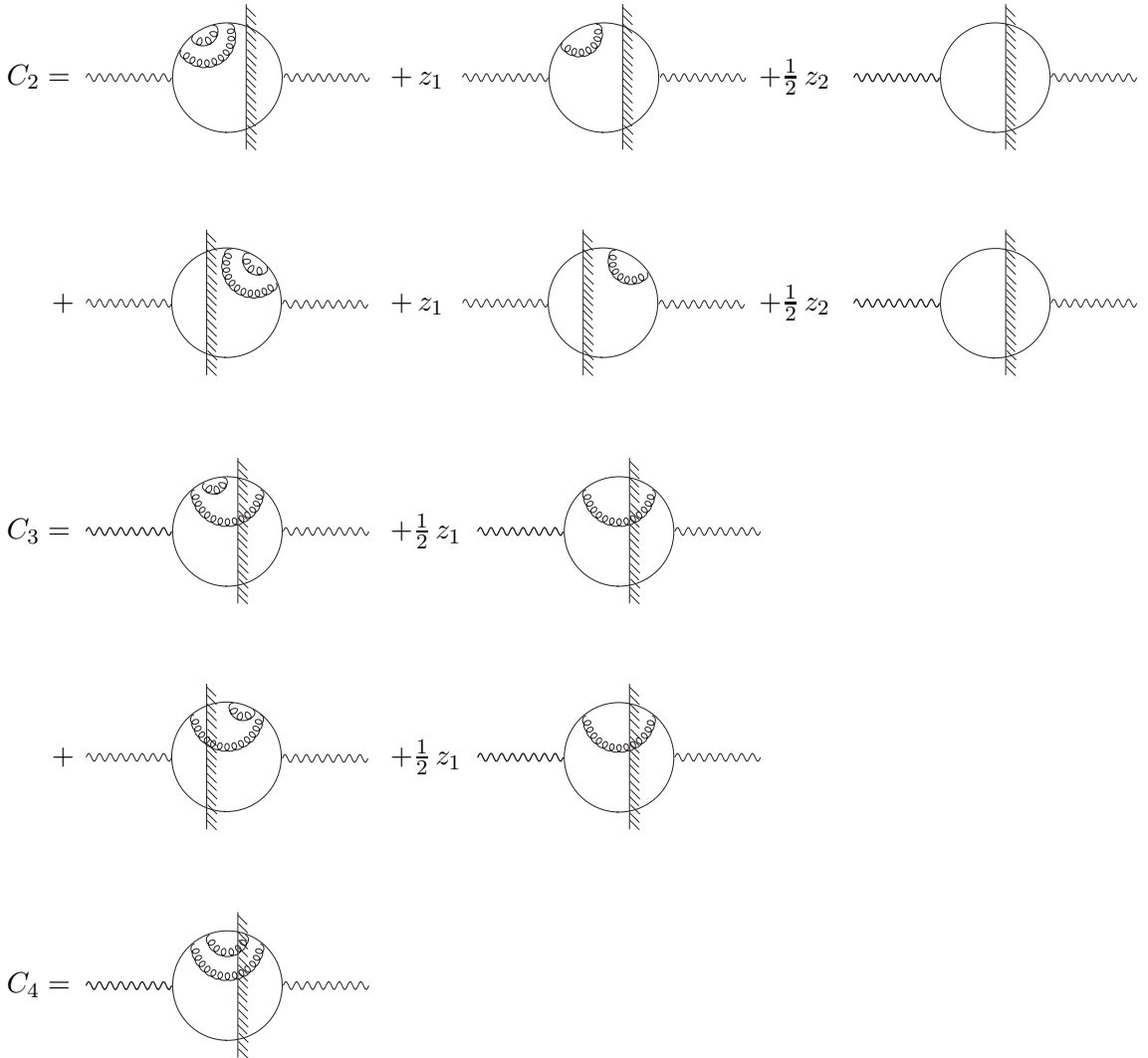
## 2 Cancellation of infrared divergences

Two-jet production in  $e^+e^-$  collisions at NNLO in  $\alpha_s$  corresponds diagrammatically to sums over cuts of three-loop vacuum polarisation graphs. After renormalization of ultraviolet subdivergences the three-loop diagram has at most an overall ultraviolet divergence with a finite imaginary part. Because this imaginary part is related to the sum over all cuts of the diagram, one concludes that the sum over all cuts has to be finite. This is just the KLN [20] cancellation mechanism for infrared final state singularities. In our case, one has 2-, 3- and 4-particle cuts which correspond to phase space integrations over the respective partons. We require 2 jets in the final state, such that up to two partons can become unresolved.

Consider for example the diagram shown in Fig. 1. In the following subsections, we will work out the UV renormalization and cut structure of this diagram. We use Feynman gauge throughout the paper.

### 2.1 Cut diagrams

Infrared cancellations take place when summing over cuts of a given renormalized topology. In our case we have the 2-, 3- and 4-particle cuts  $C_2, C_3$  and  $C_4$ , which graphically are given by



The factors  $z_1$  and  $z_2$  denote the contributions from counterterms. The sum of terms in each line in the above figures is formally UV finite. In dimensional regularization the radiative corrections to the two-point functions vanish if the particle is put on-shell. This is the mechanism which formally leads to the conversion of UV into IR poles. Using the diagrammatic rule

$$\begin{array}{ccc}
 \text{---} \text{---} \text{---} \text{---} \text{---} & = 0 \ , & \text{---} \text{---} \text{---} \text{---} \text{---} & = 0
 \end{array}$$

the only remaining terms in the sum  $C = C_2 + C_3 + C_4$  are

$$C = \text{wavy line with loop} + z_1 \text{ wavy line with loop} + z_2 \text{ wavy line with loop} \quad (1)$$

The  $1/\epsilon$  terms contained in  $z_1$  and  $z_2$  now represent IR poles. The graphs shown in (1) denote the contribution from the given topology to the full process. As the imaginary part of the corresponding 3-loop topology is finite, unitarity implies that  $C$  is IR finite.

The part which is hard to calculate analytically is the 4-particle cut, that is why we advocate a numerical evaluation of  $C_4$ . The remaining combination of counterterms and 2- and 3-particle phase space integrations can straightforwardly be done analytically. This will be worked out in the next section.

## 2.2 UV renormalization

To compute the renormalization constants  $z_1$  and  $z_2$  we have to determine the pole parts of all graphs and subgraphs. Following a graphical BPHZ notation one has to carry out the following subtractions to renormalize the one-loop selfenergy and finally the whole diagram: The one-loop subtraction:

and the two-loop subtractions:

The shaded boxes denote the  $\overline{\text{MS}}$  prescription to keep only the pole part of the expression, up to absorption of a standard factor into the coupling:

$$\alpha = C_{\overline{\text{MS}}} \alpha_0, \quad \alpha_s = C_{\overline{\text{MS}}} \alpha_{s,0}, \quad C_{\overline{\text{MS}}} = \frac{\Gamma(1 + \epsilon)(4\pi)^\epsilon}{\mu^{2\epsilon}} \quad (2)$$

Using the integral

$$\begin{aligned} I(\alpha, \beta) &= \int \frac{d^D k}{i\pi^{D/2}} \frac{\gamma^\mu k^\nu \gamma_\mu}{[-k^2]^\alpha [-(k-p)^2]^\beta} \\ &= \not{p}(2-D)(-p^2)^{D/2-\alpha-\beta} \frac{\Gamma(\alpha+\beta-D/2)}{\Gamma(\alpha)\Gamma(\beta)} \frac{\Gamma(D/2-\alpha+1)\Gamma(D/2-\beta)}{\Gamma(D-\alpha-\beta+1)} \end{aligned} \quad (3)$$

one finds the following analytic results for the graphical expressions ( $D = 4 - 2\epsilon$ ). At one loop:

$$\begin{aligned} \text{Diagram 1} &= i\not{p} C_F \left( \frac{\alpha_s}{4\pi} \right) \left( \frac{-p^2}{\mu^2} \right)^{-\epsilon} \frac{\Gamma(1-\epsilon)^2}{\Gamma(2-2\epsilon)} \frac{(1-\epsilon)}{\epsilon} \\ \text{Diagram 2} &= i\not{p} C_F \left( \frac{\alpha_s}{4\pi} \right) \frac{1}{\epsilon} \end{aligned} \quad (4)$$

and for the two-loop part:

$$\begin{aligned} \text{Diagram 3} &= -i\not{p} C_F^2 \left( \frac{\alpha_s}{4\pi} \right)^2 \left( \frac{-p^2}{\mu^2} \right)^{-2\epsilon} \frac{\Gamma(1+2\epsilon)}{\Gamma(1+\epsilon)^2} \frac{\Gamma(1-\epsilon)^3}{\Gamma(3-3\epsilon)} \frac{(1-\epsilon)^2}{\epsilon^2} \\ \text{Diagram 4} &= -i\not{p} C_F^2 \left( \frac{\alpha_s}{4\pi} \right)^2 \left( \frac{-p^2}{\mu^2} \right)^{-\epsilon} \frac{\Gamma(1-\epsilon)^2}{\Gamma(1-2\epsilon)} \frac{1-\epsilon}{\epsilon^2(1-2\epsilon)} \\ \text{Diagram 5} &= -i\not{p} C_F^2 \left( \frac{\alpha_s}{4\pi} \right)^2 \left[ \frac{1}{2\epsilon^2} + \frac{5}{4\epsilon} - \frac{1}{\epsilon} \log \left( \frac{-p^2}{\mu^2} \right) \right] \\ \text{Diagram 6} &= -i\not{p} C_F^2 \left( \frac{\alpha_s}{4\pi} \right)^2 \left[ \frac{1}{\epsilon^2} + \frac{1}{\epsilon} - \frac{1}{\epsilon} \log \left( \frac{-p^2}{\mu^2} \right) \right] \end{aligned} \quad (5)$$

The renormalization constants can be read off directly:

$$i\not{p} z_1 = \text{Diagram 2} \Rightarrow z_1 = C_F \frac{\alpha_s}{4\pi} \frac{1}{\epsilon} \quad (6)$$

$$\begin{aligned} i\not{p} z_2 &= \text{Diagram 5} - \text{Diagram 6} \\ \Rightarrow z_2 &= C_F^2 \left( \frac{\alpha_s}{4\pi} \frac{1}{\epsilon} \right)^2 \left[ \frac{1}{2} - \frac{1}{4} \epsilon \right] = \frac{1}{2} z_1^2 \left[ 1 - \frac{1}{2} \epsilon \right] \end{aligned} \quad (7)$$

The non-local logarithmic terms cancel, as guaranteed by the BPHZ theorem.

### 3 Matrix elements and phase space integrals

What remains to be done is the evaluation of the phase space integrals for the cuts shown in Eq. (1). The corresponding matrix elements are given by the following formulae, where

$p_1$  ( $p_2$ ) are the momenta of the quark (anti-quark),  $p_3$  and  $p_4$  denote the gluons.

$$|\mathcal{M}_{1 \rightarrow 2}|^2 = 16\pi \alpha (1 - \epsilon) \left( \frac{\mu^{2\epsilon}}{\Gamma(1 + \epsilon)(4\pi)^\epsilon} \right) s_{12} \quad (8)$$

$$|\mathcal{M}_{1 \rightarrow 3}|^2 = 8(4\pi)^2 (1 - \epsilon)^2 \alpha \alpha_s C_F \left( \frac{\mu^{2\epsilon}}{\Gamma(1 + \epsilon)(4\pi)^\epsilon} \right)^2 \frac{s_{23}}{s_{13}} \quad (9)$$

$$|\mathcal{M}_{1 \rightarrow 4}|^2 = 16(4\pi)^3 (1 - \epsilon)^3 \alpha \alpha_s^2 C_F^2 \left( \frac{\mu^{2\epsilon}}{\Gamma(1 + \epsilon)(4\pi)^\epsilon} \right)^3 \frac{(s_{13} + s_{34})(s_{12} + s_{24}) - s_{14}s_{23}}{s_{13}(s_{13} + s_{34} + s_{14})^2} \quad (10)$$

$|\mathcal{M}_{1 \rightarrow 2}|^2$  and  $|\mathcal{M}_{1 \rightarrow 3}|^2$  can be integrated directly. The corresponding phase space integrals are given in detail in the Appendix. We obtain

$$T_{1 \rightarrow 2} = \int d\Phi_{1 \rightarrow 2} |\mathcal{M}_{1 \rightarrow 2}|^2 = 2\alpha Q^2 \left( \frac{Q^2}{\mu^2} \right)^{-\epsilon} \frac{(1 - \epsilon)\Gamma(1 - \epsilon)}{\Gamma(1 + \epsilon)\Gamma(2 - 2\epsilon)} \quad (11)$$

Using the integral

$$J_3(\epsilon) = \int_0^\infty dy_1 dy_2 dy_3 \delta(1 - y_1 - y_2 - y_3) (y_1 y_2 y_3)^{-\epsilon} \frac{y_3}{y_2} = -\frac{(1 - \epsilon)}{\epsilon} \frac{\Gamma(1 - \epsilon)^3}{\Gamma(3 - 3\epsilon)}, \quad (12)$$

where  $y_1 = s_{12}/Q^2$ ,  $y_2 = s_{13}/Q^2$ ,  $y_3 = s_{23}/Q^2$ , one finds for the  $1 \rightarrow 3$  case:

$$\begin{aligned} T_{1 \rightarrow 3} &= \int d\Phi_{1 \rightarrow 3} |\mathcal{M}_{1 \rightarrow 3}|^2 \\ &= \alpha \alpha_s C_F \frac{(2\pi)^{2\epsilon}}{8\pi^3} (1 - \epsilon)^2 Q^2 \left( \frac{Q^2}{\mu^2} \right)^{-2\epsilon} \frac{V(3 - 2\epsilon) V(2 - 2\epsilon)}{\Gamma(1 + \epsilon)^2} J_3(\epsilon) \\ &= -z_1 T_{1 \rightarrow 2} \left( \frac{Q^2}{\mu^2} \right)^{-\epsilon} \frac{2(1 - \epsilon)^2 \Gamma(1 - \epsilon)^2}{\Gamma(1 + \epsilon) \Gamma(3 - 3\epsilon)} \end{aligned} \quad (13)$$

The  $1 \rightarrow 4$  case cannot be solved easily analytically. We write it in the following form:

$$\begin{aligned} T_{1 \rightarrow 4} &= \int d\Phi_{1 \rightarrow 4} |\mathcal{M}_{1 \rightarrow 4}|^2 \\ &= (z_1 \epsilon)^2 T_{1 \rightarrow 2} \left( \frac{Q^2}{\mu^2} \right)^{-2\epsilon} \frac{(1 - \epsilon)^2}{\Gamma(1 + \epsilon)^2 \Gamma(1 - 2\epsilon)} J_4(\epsilon) \end{aligned} \quad (14)$$

where the nontrivial integral  $J_4(\epsilon)$  remains, which will be dealt with numerically in the next section.

So far, one finds for the cut diagrams in Eq. (1):

$$C_2 = z_1^2 T_{1 \rightarrow 2} \left( \frac{1}{2} - \frac{1}{4}\epsilon \right)$$

$$\begin{aligned}
C_3 &= -z_1^2 T_{1 \rightarrow 2} \left( \frac{Q^2}{\mu^2} \right)^{-\epsilon} (1-\epsilon)^2 \left[ 1 + \frac{9}{2}\epsilon + \epsilon^2 \left( \frac{63}{4} - \frac{2\pi^2}{3} \right) + \mathcal{O}(\epsilon^3) \right] \\
C_4 &= z_1^2 T_{1 \rightarrow 2} \left( \frac{Q^2}{\mu^2} \right)^{-2\epsilon} \epsilon^2 (1-\epsilon)^2 \left[ 1 - \epsilon^2 \frac{\pi^2}{2} + \mathcal{O}(\epsilon^3) \right] J_4(\epsilon)
\end{aligned} \tag{15}$$

and consequently the poles contained in  $J_4(\epsilon)$  have to cancel with

$$(C_2 + C_3)|_{\text{pole part}} = z_1^2 T_{1 \rightarrow 2} \left[ -\frac{1}{2} - \frac{11}{4}\epsilon + \epsilon \log \left( \frac{Q^2}{\mu^2} \right) \right]. \tag{16}$$

## 4 Numerical evaluation of $1 \rightarrow 4$ phase space integrals

In massless QCD, the integrals of any  $1 \rightarrow 4$  matrix element over the total phase space can be expressed by four master integrals whose analytical evaluation is complicated, but has been achieved in [15]. This allows to follow the conventional procedure to establish a subtraction scheme and to integrate the subtraction terms analytically. However, as the finite part of the phase space will finally be integrated numerically anyway, a flexible, completely numerical method would be welcome. Of course the problem consists in the isolation and subtraction of the infrared poles, stemming from the integration over unresolved particles, before a numerical evaluation is possible. This is where sector decomposition is very convenient. How it proceeds is shown for the sample integral  $J_4$  defined in eq. (17). Note that this integral contains an integrable singularity of square-root type. For the sake of numerical stability it is preferable to perform a mapping such that the integrand is bounded near the phase space limits. In detail we proceed as follows:

Our starting point is the integral  $J_4(\epsilon)$  which represents (up to an overall factor, see eqs. (10),(15)) the integral over the 4-particle cut of the topology in Fig. 1.

$$J_4(\epsilon) = \frac{4}{\pi} \int_0^\infty \prod_{i=1}^6 dy_i \Theta(-\lambda)(-\lambda)^{-1/2-\epsilon} \delta(1 - \sum_{j=1}^6 y_j) \frac{(y_1 + y_5)(y_2 + y_6) - y_3 y_4}{y_2 (y_2 + y_4 + y_6)^2}, \tag{17}$$

where we have rescaled the Mandelstam invariants by

$$y_1 = s_{12}/Q^2, y_2 = s_{13}/Q^2, y_3 = s_{23}/Q^2, y_4 = s_{14}/Q^2, y_5 = s_{24}/Q^2, y_6 = s_{34}/Q^2$$

and  $\lambda \equiv \lambda(y_1 y_6, y_2 y_5, y_3 y_4)$  is the Källen function  $\lambda(x, y, z) = x^2 + y^2 + z^2 - 2xy - 2yz - 2xz$ . The derivation of the phase space integral can be found in the appendix, see eq. (37).

### Primary sector decomposition

To eliminate the delta distribution in (17) we split the integration region into 6 "primary sectors" by the following decomposition of unity:

$$1 = \sum_{j=1}^6 \prod_{k \neq j=1}^6 \Theta(y_j - y_k) \tag{18}$$

In each primary sector  $j$  we apply the mapping

$$y_k = \begin{cases} t_k y_j & \text{if } k \neq j \\ y_j & \text{if } k = j \end{cases} \quad (19)$$

Note that to each index there exists a conjugate index defined by the pairing of Mandelstam variables in the arguments of the Källen function,  $\lambda(y_1 y_6, y_2 y_5, y_3 y_4)$ . The constraint  $\Theta(-\lambda)$  is solved for the variable with index conjugate to  $j$  in each primary sector  $j$ . To be explicit we give the result for primary sector 1 in the following, where we have

$$\lambda(t_6, t_2 t_5, t_3 t_4) = 0 \Leftrightarrow t_6^\pm = t_2 t_5 + t_3 t_4 \pm 2\sqrt{t_2 t_3 t_4 t_5} = (\sqrt{t_2 t_5} \pm \sqrt{t_3 t_4})^2$$

### Remapping the square-root singularity

Before iterated sector decomposition can be applied to disentangle the IR singularities, it is necessary to perform some variable transformations such that finally all possible singularities are at zero. Further it is useful to make a quadratic transformation  $t_j = x_j^2$  for  $j = 2, 3, 4, 5$  to avoid square roots.

One possibility of remapping is to split each primary sector into two subsectors A and B, with  $t_6 \in [t_6^-, t_6^+] = A$  and  $t_6 \in [t_6^0, t_6^+] = B$ , where  $t_6^0 = t_2 t_5 + t_3 t_4$ . The following transformations then lead to a numerically stable behaviour near the phase-space boundaries:

$$\begin{aligned} t_6^A &= t_6^- + (t_6^0 - t_6^-) x_6^2 = (x_2 x_5 - x_3 x_4)^2 + 2x_2 x_3 x_4 x_5 x_6^2 \\ t_6^B &= t_6^+ - (t_6^+ - t_6^0) x_6^2 = (x_2 x_5 + x_3 x_4)^2 - 2x_2 x_3 x_4 x_5 x_6^2 \end{aligned} \quad (20)$$

After these transformations the integral  $J_{4,\text{sec1}}$  in primary sector one is given by

$$\begin{aligned} J_{4,\text{sec1}} &= \frac{4}{\pi} (J_{4,1}^A + J_{4,1}^B) \\ J_{4,1}^{A,B} &= 2^{5-2\epsilon} \int_0^1 \prod_{j=2}^6 dx_j (x_2 x_3 x_4 x_5)^{1-2\epsilon} x_6^{-2\epsilon} (2 - x_6^2)^{-1/2-\epsilon} \Theta(1 - t_6^{A,B}(\vec{x})) \\ &\quad \times F(1, x_2^2, x_3^2, x_4^2, x_5^2, t_6^{A,B}(\vec{x})) \end{aligned} \quad (21)$$

The function  $F$  depends on the topology, in our case

$$F(z_1, \dots, z_6) = \left( \sum_{j=1}^6 z_j \right)^{-3+4\epsilon} \frac{(z_1 + z_5)(z_2 + z_6) - z_3 z_4}{z_2(z_2 + z_4 + z_6)^2}. \quad (22)$$

Note that the  $\Theta$ -function constraint is trivially fulfilled whenever one of the variables  $x_j$ ,  $j \in \{2, 3, 4, 5\}$  goes to zero. However, at this point we have not mapped all possible singularities to zero yet. For example,  $t_6^A$  can vanish if  $\{x_2, x_3, x_4, x_5\} \rightarrow 1, x_6 \rightarrow 0$ . In this case another transformation  $x_j \rightarrow 1 - x_j$  is made<sup>1</sup>. Note that all these transformations are done automatically in our program. Having finally mapped all possible singularities to zero, iterated sector decomposition can be applied straightforwardly. One obtains the coefficients of the  $1/\epsilon$  poles as finite parameter integrals which can be integrated numerically, in the same way as has been explained in [15, 16].

<sup>1</sup>It can occur that  $x_j \rightarrow 0$  is singular as well for some  $j \in \{2, 3, 4, 5\}$ . In this case the integration region for  $x_j$  is split at  $1/2$ , and only after this splitting the variables are remapped such that all possible singularities are located at zero.

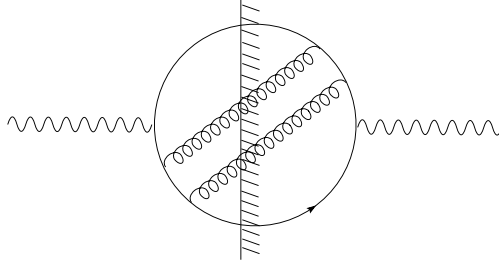


Figure 2: Cut topology with  $1/\epsilon^4$  poles.

## Numerical solution

For the integral  $J_4$  we find numerically

$$(1 - \epsilon)^2 J_4 = 0.500 \frac{1}{\epsilon^2} + 2.749 \frac{1}{\epsilon} + 7.869 + \mathcal{O}(\epsilon) \quad (23)$$

Inserting this result into (15) and comparing to eq. (16) we see that the poles are cancelled within the numerical precision which we chose to be 0.1%.

## 5 Another Topology

To show that our method also works in the case of a more complicated pole structure and a lengthier numerator, we consider now the cut graph shown in Fig. 2, which leads to poles up to  $1/\epsilon^4$ , and the expanded numerator contains about 70 terms. The corresponding matrix element is given by ( $p_{ij\dots} = p_i + p_j + \dots$ )

$$|\mathcal{M}_{1 \rightarrow 4}|^2 = -(4\pi)^3 \alpha \alpha_s^2 C_F^2 \left( \frac{\mu^{2\epsilon}}{\Gamma(1+\epsilon)(4\pi)^\epsilon} \right)^3 \frac{\text{tr}(p_1 \gamma^\sigma p_{13} \gamma^\rho p_{134} \gamma^\mu p_2 \gamma_\rho p_{24} \gamma_\sigma p_{234} \gamma_\mu)}{s_{134} s_{13} s_{234} s_{24}} \quad (24)$$

Writing again the phase space integral in the form

$$\tilde{T}_{1 \rightarrow 4} = \int d\Phi_{1 \rightarrow 4} |\mathcal{M}_{1 \rightarrow 4}|^2 = (z_1 \epsilon)^2 T_{1 \rightarrow 2} \left( \frac{Q^2}{\mu^2} \right)^{-2\epsilon} \frac{1}{16(1-\epsilon)\Gamma(1+\epsilon)^2\Gamma(1-2\epsilon)} \tilde{J}_4(\epsilon)$$

we obtain numerically

$$\tilde{J}_4 = \frac{1.000}{\epsilon^4} + \frac{3.000}{\epsilon^3} + \frac{3.776}{\epsilon^2} + \frac{8.957}{\epsilon} + 57.85 + \mathcal{O}(\epsilon) \quad (25)$$

We stress that no analytical manipulations whatsoever, in particular no reduction to master integrals, are necessary to achieve this result.

## 6 Discussion and Outlook

In this paper we have argued that the method of sector decomposition as proposed in [18, 15] and applied in a similar form in [19] can serve to calculate the double real emission part

needed for NNLO corrections to jet cross sections in massless QCD. We have shown explicitly how the IR poles cancel by considering one sample topology contributing to  $e^+e^- \rightarrow 2$  jets at NNLO. We calculated all cuts contributing to a 2 jet final state: The double real emission part, corresponding to a 4-particle cut, is calculated numerically by sector decomposition, and all the poles are shown to cancel with contributions from the 2-and 3-particle cuts within the chosen numerical precision<sup>2</sup>. We also calculated numerically the 4-particle cut of a topology which has the maximal possible number of IR poles.

The method has several appealing features:

- The (overlapping) soft/collinear poles are extracted without the need to establish a subtraction scheme and to integrate analytically over complicated subtraction terms.
- The finite parts are available as regular functions of the kinematic invariants. If a measurement function is included, as already has been done in [19], one can obtain fully differential cross sections, such that for example the implementation of experimental cuts should be straightforward.
- It is justified to expect that the Monte Carlo integration to obtain the final cross section does not lead to major instabilities as the singularities at phase space boundaries already have been remapped.
- The generalisation of the method to the  $1 \rightarrow 5$  phase space is feasible but has to be investigated further.

The complete double real emission part contributing to  $e^+e^- \rightarrow 2$  jets can be evaluated along the same lines and will be given elsewhere.

## Acknowledgement

We would like to thank the Kavli Institute for Theoretical Physics for its kind hospitality while part of this work has been completed. This research was supported in part by the National Science Foundation under Grant No. PHY99-07949.

## Appendix

### The D-dimensional $1 \rightarrow N$ phase space for $N = 2, 3, 4$

The differential form of the phase space for a  $1 \rightarrow N$  particle phase space in  $D$  dimensions is given by

$$d\Phi_{1 \rightarrow N} = (2\pi)^{N-D(N-1)} \left[ \prod_{j=1}^N d^D p_j \delta(p_j^2) \Theta(E_j) \right] \delta(Q - \sum_{j=1}^N p_j) \quad (26)$$

Here  $Q$  is the incoming momentum and the  $p_j$  denote outgoing particles with light-like momenta and energy component  $E_j$ . As  $Q$  is time-like for physical kinematics one can always achieve  $Q = (E, \vec{0}^{(D-1)})$  by an adequate Lorentz boost. Let us specialise now to the cases  $N = 2, 3, 4$ .

---

<sup>2</sup>Note that the method of sector decomposition could also serve to calculate the 2-and 3-particle cut contributions. In this case the algorithm for multi-loop integrals as described in [16, 17] can be applied.

**Case 1 → 2:**

For  $N = 2$  the momenta can be parametrized by

$$Q = (E, \vec{0}^{(D-1)}) , p_1 = E_1 (1, \vec{0}^{(D-2)}, 1) , p_2 = Q - p_1 \quad (27)$$

Integrating out the  $\delta$ -distributions leads to

$$d\Phi_{1 \rightarrow 2} = (2\pi)^{2-D} 2^{1-D} (Q^2)^{D/2-2} d\Omega_{D-2} \quad (28)$$

where  $d\Omega_{D-2}$  is the differential surface element of the  $S_{D-2}$  sphere. Its integral is equal to the volume of the  $(D-1)$ -dimensional unit sphere

$$\int_{S_{D-2}} d\Omega_{D-2} = V(D-1) = \frac{2\pi^{\frac{D-1}{2}}}{\Gamma(\frac{D-1}{2})} \quad (29)$$

**Case 1 → 3:**

For  $N = 3$  one can choose a coordinate frame such that

$$\begin{aligned} Q &= (E, \vec{0}^{(D-1)}) \\ p_1 &= E_1 (1, \vec{0}^{(D-2)}, 1) \\ p_2 &= E_2 (1, \vec{0}^{(D-3)}, \sin \theta, \cos \theta) \\ p_3 &= Q - p_2 - p_1 \end{aligned} \quad (30)$$

Integrating out the  $\delta$ -distributions yields

$$d\Phi_{1 \rightarrow 3} = \frac{1}{4} (2\pi)^{3-2D} dE_1 dE_2 d\theta_1 [E_1 E_2 \sin \theta]^{D-3} d\Omega_{D-2} d\Omega_{D-3} \quad (31)$$

As in the following a parametrization in terms of the Mandelstam variables  $s_{ij} = 2 p_i \cdot p_j$  will be useful, we make the transformation  $E_1, E_2, \theta \rightarrow s_{12}, s_{23}, s_{13}$ . To work with dimensionless variables we define  $y_1 = s_{12}/Q^2$ ,  $y_2 = s_{13}/Q^2$ ,  $y_3 = s_{23}/Q^2$  which leads to

$$\begin{aligned} d\Phi_{1 \rightarrow 3} &= (2\pi)^{3-2D} \frac{2^{4-D}}{32} (Q^2)^{D-3} d\Omega_{D-2} d\Omega_{D-3} [y_1 y_2 y_3]^{D/2-2} \\ &\quad dy_1 dy_2 dy_3 \Theta(y_1) \Theta(y_2) \Theta(y_3) \delta(1 - y_1 - y_2 - y_3) \end{aligned} \quad (32)$$

**Case 1 → 4:**

Starting from Eq. (26) and eliminating  $p_4$  yields

$$\begin{aligned} d\Phi_{1 \rightarrow 4} &= (2\pi)^{4-3D} \frac{d^{D-1} p_1}{2 E_1} \frac{d^{D-1} p_2}{2 E_2} \frac{d^{D-1} p_3}{2 E_3} \Theta(E_1) \Theta(E_2) \Theta(E_3) \\ &\quad \Theta(E - E_1 - E_2 - E_3) \delta((Q - p_1 - p_2 - p_3)^2) \end{aligned} \quad (33)$$

Choosing a frame where

$$\begin{aligned}
Q &= (E, \vec{0}^{(D-1)}) \\
p_1 &= E_1 (1, \vec{0}^{(D-2)}, 1) \\
p_2 &= E_2 (1, \vec{0}^{(D-3)}, \sin \theta_1, \cos \theta_1) \\
p_3 &= E_3 (1, \vec{0}^{(D-4)}, \sin \theta_3 \sin \theta_2, \cos \theta_3 \sin \theta_2, \cos \theta_2) \\
p_4 &= Q - p_1 - p_2 - p_3 .
\end{aligned} \tag{34}$$

leads to

$$\begin{aligned}
d\Phi_{1 \rightarrow 4} &= \frac{1}{8} (2\pi)^{4-3D} dE_1 dE_2 dE_3 d\theta_1 d\theta_2 d\theta_3 [E_1 E_2 E_3 \sin \theta_1 \sin \theta_2]^{D-3} \sin \theta_3^{D-4} \\
&\quad d\Omega_{D-2} d\Omega_{D-3} d\Omega_{D-4} \Theta(E_1) \Theta(E_2) \Theta(E_3) \Theta(E - E_1 - E_2 - E_3) \\
&\quad \delta(E^2 - 2E(E_1 + E_2 + E_3) + 2(p_1 \cdot p_2 + p_1 \cdot p_3 + p_2 \cdot p_3))
\end{aligned} \tag{35}$$

As above we map the angle and energy variables to the Mandelstam invariants as integration variables. The Jacobian in combination with terms already present in (35) can be written as the determinant of the Gram matrix  $G_{ij} = 2 p_i \cdot p_j$ . The determinant can be expressed by the Källen function  $\lambda(x, y, z) = x^2 + y^2 + z^2 - 2xy - 2yz - 2xz$  as

$$\begin{aligned}
\det(G) &= \lambda(s_{12} s_{34}, s_{13} s_{24}, s_{14} s_{23}) \\
&= -[4 E E_1 E_2 E_3 \sin \theta_1 \sin \theta_2 \sin \theta_3]^2
\end{aligned} \tag{36}$$

We see that  $\det(G)$  has to be negative semi-definite. With the dimensionless variables

$$y_1 = s_{12}/Q^2, y_2 = s_{13}/Q^2, y_3 = s_{23}/Q^2, y_4 = s_{14}/Q^2, y_5 = s_{24}/Q^2, y_6 = s_{34}/Q^2$$

and  $\lambda = \lambda(y_1 y_6, y_2 y_5, y_3 y_4)$  one obtains finally

$$\begin{aligned}
d\Phi_{1 \rightarrow 4} &= (2\pi)^{4-3D} (Q^2)^{3D/2-4} 2^{-2D+1} d\Omega_{D-2} d\Omega_{D-3} d\Omega_{D-4} \\
&\quad \left[ \prod_{j=1}^6 dy_j \Theta(y_j) \right] \Theta(-\lambda) [-\lambda]^{(D-5)/2} \delta(1 - \sum_{j=1}^6 y_j)
\end{aligned} \tag{37}$$

## References

- [1] Z. Bern, L.J. Dixon and A. Ghinculov, Phys. Rev. D **63** (2001) 053007 [hep-ph/0010075];  
Z. Bern, A. De Freitas, L.J. Dixon, A. Ghinculov and H.L. Wong, JHEP **0111** (2001) 031 [hep-ph/0109079];  
Z. Bern, A. De Freitas and L.J. Dixon, JHEP **0109** (2001) 037 [hep-ph/0109078]; JHEP **0203** (2002) 018 [hep-ph/0201161]; JHEP **0306** (2003) 028 [hep-ph/0304168].
- [2] C. Anastasiou, E.W.N. Glover, C. Oleari and M.E. Tejeda-Yeomans, Nucl. Phys. B **601** (2001) 318 [hep-ph/0010212]; **601** (2001) 347 [hep-ph/0011094]; **605** (2001) 486 [hep-ph/0101304];  
E.W.N. Glover, C. Oleari and M.E. Tejeda-Yeomans, Nucl. Phys. **605** (2001) 467

[hep-ph/0102201];  
 C. Anastasiou, E.W.N. Glover and M.E. Tejeda-Yeomans, Nucl. Phys. B **629** (2002) 255 [hep-ph/0201274];  
 T. Binoth, E.W.N. Glover, P. Marquard and J.J. van der Bij, JHEP **0205** (2002) 060 [hep-ph/0202266];  
 E.W.N. Glover and M.E. Tejeda-Yeomans, JHEP **0306** (2003) 033 [hep-ph/0304169].

[3] L.W. Garland, T. Gehrmann, E.W.N. Glover, A. Koukoutsakis and E. Remiddi, Nucl. Phys. B **627** (2002) 107 [hep-ph/0112081] and **642** (2002) 227 [hep-ph/0206067].

[4] S. Moch, P. Uwer and S. Weinzierl, Phys. Rev. D **66** (2002) 114001 [hep-ph/0207043].

[5] T. Gehrmann and E. Remiddi, Nucl. Phys. B **640** (2002) 379 [hep-ph/0207020].

[6] E. W. N. Glover, arXiv:hep-ph/0401119.

[7] Z. Bern, L.J. Dixon, D.C. Dunbar and D.A. Kosower, Nucl. Phys. B **425** (1994) 217 [hep-ph/9403226];  
 D.A. Kosower, Nucl. Phys. B **552** (1999) 319 [hep-ph/9901201];  
 D.A. Kosower and P. Uwer, Nucl. Phys. B **563** (1999) 477 [hep-ph/9903515];  
 Z. Bern, V. Del Duca and C.R. Schmidt, Phys. Lett. B **445** (1998) 168 [hep-ph/9810409];  
 Z. Bern, V. Del Duca, W.B. Kilgore and C.R. Schmidt, Phys. Rev. D **60** (1999) 116001 [hep-ph/9903516];  
 S. Catani and M. Grazzini, Nucl. Phys. B **591** (2000) 435 [hep-ph/0007142].

[8] D.A. Kosower, Phys. Rev. Lett. **91** (2003) 061602 [hep-ph/0301069].

[9] S. Weinzierl, JHEP **0307** (2003) 052 [hep-ph/0306248].

[10] J. Campbell and E.W.N. Glover, Nucl. Phys. B **527** (1998) 264 [hep-ph/9710255];  
 S. Catani and M. Grazzini, Phys. Lett. B **446** (1999) 143 [hep-ph/9810389]; Nucl. Phys. B **570** (2000) 287 [hep-ph/9908523];  
 F.A. Berends and W.T. Giele, Nucl. Phys. B **313** (1989) 595.

[11] D. A. Kosower, Phys. Rev. D **67** (2003) 116003 [hep-ph/0212097].

[12] S. Weinzierl, JHEP **0303** (2003) 062 [hep-ph/0302180].

[13] A. Gehrmann-De Ridder, T. Gehrmann and E.W.N. Glover, “Radiative corrections to the photon + 1jet rate at LEP,” Phys. Lett. B **414** (1997) 354 [hep-ph/9705305].

[14] A. Gehrmann-De Ridder and E.W.N. Glover, Nucl. Phys. B **517** (1998) 269 [hep-ph/9707224].

[15] A. Gehrmann-De Ridder, T. Gehrmann and G. Heinrich, arXiv:hep-ph/0311276.

[16] T. Binoth and G. Heinrich, Nucl. Phys. B **585** (2000) 741 [hep-ph/0004013].

[17] T. Binoth and G. Heinrich, Nucl. Phys. B **680** (2004) 375 [hep-ph/0305234].

- [18] G. Heinrich, Nucl. Phys. Proc. Suppl. **116** (2003) 368 [hep-ph/0211144].
- [19] C. Anastasiou, K. Melnikov and F. Petriello, arXiv:hep-ph/0311311.
- [20] T. Kinoshita, J. Math. Phys. **3** (1962) 650;  
T. D. Lee and M. Nauenberg, Phys. Rev. **133** (1964) B1549.